

EFFECTS OF TRANSIENT PROPELLANT DYNAMICS ON DEPLOYMENT OF  
LARGE LIQUID STAGES IN ZERO-GRAVITY WITH  
APPLICATION TO SHUTTLE/CENTAUR

R.E. Martin

General Dynamics Space Systems Division  
San Diego, California, USA

ABSTRACT

A common requirement of the space station era will be deployment and docking of orbit transfer vehicles with large quantities of liquid propellants. The maneuver will typically start at zero gravity with short, transient accelerations applied to provide accurate vehicle positioning for clearance during deployment or engagement during docking. Since the propellant tanks are not always full and the initial zero-g position of liquid and ullage may not be known, transient fluid forces can have a major influence on vehicle motion. Until recently, this fluid dynamics problem could not be analyzed adequately. This paper describes the application of a recently developed computational fluid dynamics (CFD) program, HYDR-3D, to the analysis of separation of the Centaur G-Prime vehicle from the Space Shuttle Orbiter. The typical application presented illustrates a particularly difficult design task - deployment of a large, liquid-filled, densely packaged vehicle from a manned vehicle. Since it represents a potential catastrophic hazard, a vast number of conditions and parameters must be analyzed to ensure tolerance of at least two credible failures. Validation of the HYDR-3D program against zero- and low-gravity experimental data is also presented. Using the fluid dynamics program, this approach can be used confidently to analyze and determine design requirements for a variety of orbit transfer vehicle/space station deployment and docking problems.

KEYWORDS

Space vehicle deployment; upper stage separation; zero-gravity fluid dynamics; computational fluid dynamics; Shuttle/Centaur.

CENTAUR/ORBITER SEPARATION SYSTEM

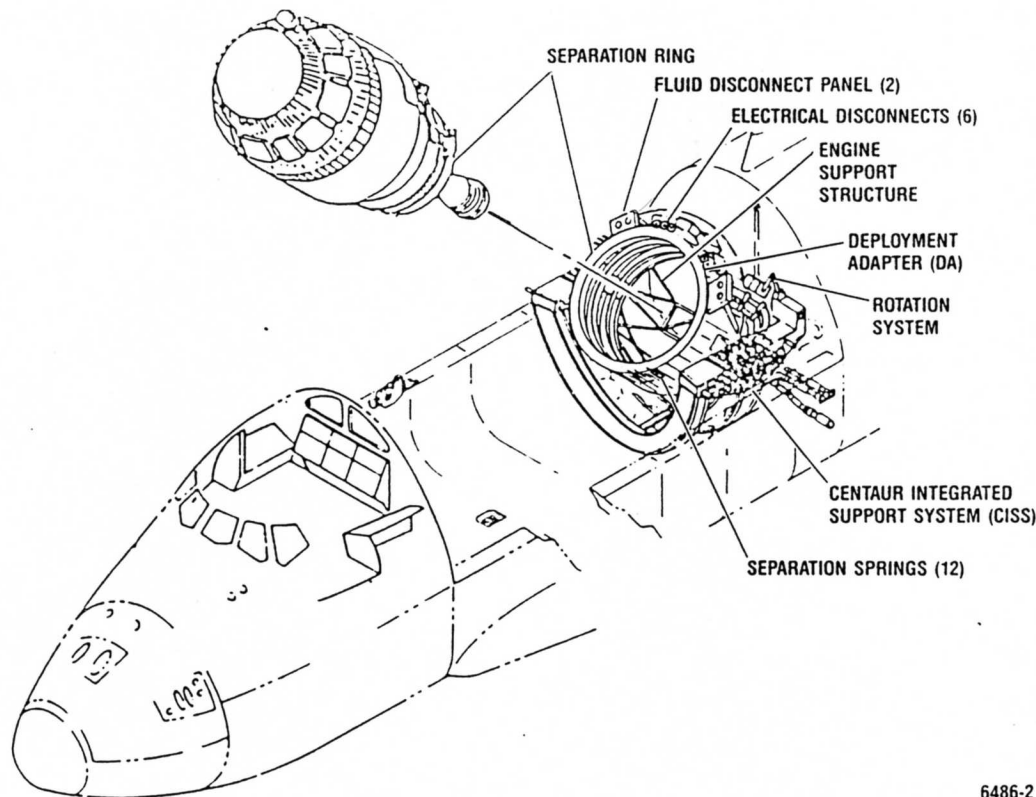
The Centaur G-Prime is a modification of the  $LO_2/LH_2$  fueled Centaur that has flown as an upper stage on Atlas and Titan launch vehicles since 1962. Designed for full use of the Orbiter payload bay volume, it provides maximum possible synchronous orbit and planetary mission performance with state-of-the art propulsion. A schematic of its separation from the Orbiter is shown in Fig. 1. Until cancelled in the wake of the Challenger accident, the G-Prime had been the first large liquid stage scheduled to fly from the Shuttle in May 1986. A version of G-Prime is now planned as an upper stage for Titan for use on high energy missions. The first two missions, planned for the Shuttle, Galileo and Ulysses, are used in this paper to illustrate effects of propellant dynamics on deployment of a large liquid stage in zero-g and the methodology for analyzing the problem this presents. On Ulysses, for example, the  $LO_2$  weight of 37,500 lb. is 71 percent of the total separated weight of 52,600 lb. It is obvious that  $LO_2$  motion and forces on the tank must be accurately predicted in order to determine vehicle motion.

For separation, the Centaur is rotated 45 degrees out of the Orbiter bay by a rotation system driving the deployment adapter (DA). Separation is initiated by a Super\*Zip ring, which circumferentially severs the Centaur aft adapter from the DA. Separation force is provided by 12 compressed coil springs plus a number of spring-loaded disconnects. The springs have a 4-inch stroke; the disconnects have 2.2 inches or less. Maximum axial acceleration is about 0.1g, with a minimum relative separation velocity of 1 ft/sec. Four 11-inch-long guides alleviate angular motion resulting from any imbalances in the separation forces, but are not long enough to control all residual effects of propellant motion. The critical clearance is that between the engine bell and the DA. The aft end of the bell must travel 93 inches before it clears the DA and about 60 feet before it clears the Orbiter cabin.

HYDR-3D PROPELLANT DYNAMICS ANALYSIS APPROACH

The most difficult aspect of ensuring adequate clearance is determining the transient propellant forces on the tanks resulting from impulsive separation and guide forces. Because of its weight,  $LO_2$  is the largest factor. The 45-degree deployment and the Orbiter attitude control create tank accelerations of about  $10^{-6}g$ , even before separation. This causes the spherical zero-g ullage bubble to become ellipsoidal and to be located almost any place in the tank at the instant of separation. Scale-model drop-tower tests by the NASA/Lewis Research Center (Carney, 1985) showed that a stable, centered ullage location existed only for low-liquid-fill levels of less than about 40%. Above 80% fill, the ullage bubbles were small enough to be accommodated anywhere within the container boundaries. As bubble diameter increased for fills less than 80%, the tendency for the bubble to attach to the desired wall with largest radius of curvature increased.

Most missions desire maximum propellant fill, which is about 96%. This has the most uncertainty of ullage location but the least effect from it. However, several factors (e.g., trajectory, energy, Shuttle lift capability, stay-time before deployment) result in fill levels in the 65 to 96% range. The lower the fill, the larger the effect on separation, and the ullage location is still uncertain. Most likely, then, the propellant center of mass will be offset from the axial centerline and the axial separation acceleration will cause rotation of the propellants. The resulting moments and lateral forces have a major effect on vehicle motion and DA clearance.



6486-2

Fig. 1. Shuttle/Centaur separation system.

A recently available large-scale CFD computer program, HYDR-3D, developed by Flow Science, Inc., was the only method found to determine propellant dynamic forces for the conditions imposed. Key features of the program are listed in Table 1 and a full description and user instructions are furnished by Hirt and Sicilian (1985a). HYDR-3D has evolved from the well-known Marker-and-Cell finite difference technique which uses pressure and velocity as primary dependent variables. It is a general, three-dimensional hydrodynamics code which solves the Navier-Stokes equations of an incompressible (or slightly compressible) fluid with multiple free surfaces. Forces and moments are calculated by summing the pressure-area product for each cell in the computational mesh. General tank geometry may be modelled, including internal parts that may be modelled as either solid obstructions or porous baffles.

Table 1. HYDR-3D program description.

<ul style="list-style-type: none"> <li>— General-purpose, finite-difference, large-scale computational fluid dynamics program developed by Flow Science, Inc.</li> <li>— 3D Navier-Stokes dynamics including surface tension, wall viscous forces &amp; limited compressibility</li> <li>— Fractional area/volume method for obstacles</li> <li>— General free surface configurations</li> <li>— Multiple boundary conditions</li> <li>— Variable mesh</li> <li>— Automatic time-step (stability) controls</li> <li>— General non-inertial accelerations</li> <li>— Mesh, fluid region, baffle &amp; obstacle generators</li> <li>— Extensive graphics output of flow velocity patterns, net fluid forces &amp; moments on tank walls</li> </ul>
--

6486-3

This capability for handling three-dimensional, real-vehicle, complex geometry and general liquid/ullage interface geometry is believed to be unique. It eliminates the need for gross idealization of fluid dynamics in real tank shapes, similarly to what large-scale finite-element programs have done for structural analysis. Hirt and Sicilian (1985b) present, in detail, the variable porosity technique for obstacles in the flow path, Fractional Area Volume Obstacle Representation (FAVOR). They also discuss methods of avoiding grid distortion and numerical instability and accuracy problems and reasons for using a finite difference rather than a finite element approach.

The mesh can be varied to use small cells in areas of high dynamic activity and large cells in less active areas. Typical cell distributions mesh for the G-Prime LO<sub>2</sub> tank is shown in Fig. 7 and 9. The tank is an oblate spheroid with a cylindrical midsection. It contains a midsection solid ring and a porous, internal thrust barrel at the aft end which are important to internal tank fluid motion. The direction and magnitude of velocity for each cell containing liquid are portrayed by the arrows. Any cross-section in any direction may be displayed, as well as three-dimensional representations. Pressure distributions may also be displayed.

HYDR-3D also models wall wiping viscous effects and fluid surface-tension effects. For full-scale 3D analyses, typically 6,000 cells are used to model the LO<sub>2</sub> tank. For small-scale experimental models where surface tension cannot be fully scaled and is much more significant, 16,000 cells have been required. The code contains many good, user-oriented features such as automatic mesh generation, automatic time step control, and extensive graphics output of flow velocity, pressure patterns, and net fluid forces and moments on tank walls.

#### INTEGRATED SEPARATION ANALYSIS

To obtain the desired end result of vehicle motion it was necessary to combine the rigid body separation program (SEP) with HYDR-3D. SEP is a vehicle-peculiar program which contains six rigid-body degrees of freedom for Centaur and for the Orbiter, free-play and elastic clockspring representing the rotation system, force/stroke characteristics of each separation spring and disconnect, guide gap and flexibility, and forces and moments representing a root-sum-square of the worst-case tolerances of each spring and disconnect. The Orbiter on-orbit attitude control system is also included to evaluate pre-separation loads and its potential value for settling the propellants. For coupled analysis SEP (using inertia properties representing Centaur with an empty LO<sub>2</sub> tank) is inserted as a subroutine in HYDR-3D. Spring, disconnect, guide, and fluid force are input to SEP, and vehicle motion and tank accelerations are output. The tank accelerations are input to HYDR-3D, which calculates the net forces and moments on the tank walls, which are input back to SEP each integration time step. The other forces are updated within SEP.

The flow diagram of the integrated analysis program is shown in Fig. 2. Satisfactory numerical stability and accuracy were obtained only after some difficulty. Initially, the straightforward technique successfully used by Rocketdyne (Estes, Chang, Hirt, and Sicilian, 1985) in the coast phase control dynamics model of a liquid upper stage was attempted. In their approach, both the fluid dynamics model (SOLA-SLOSH, an earlier version of HYDR-3D) and the vehicle dynamic model integrate their respective state variables forward in time, passing hydrodynamic forces and moments from SOLA to the vehicle model and passing vehicle accelerations and angular velocities from the vehicle model back to SOLA. This approach often produced numerical instabilities in the Centaur application. Moreover, reduction of time integration step size, the traditional method of correcting integration instability, was found to be useless in correcting the divergence. At this point a simplified analysis by Dr. Jim Sicilian of Flow Sciences showed that the coupled system is inherently numerically unstable if the liquid mass is greater than 50 percent of the total. Significantly, the Rocketdyne liquid mass was about 20 percent whereas the Centaur applications are near, or greater than, 50 percent.

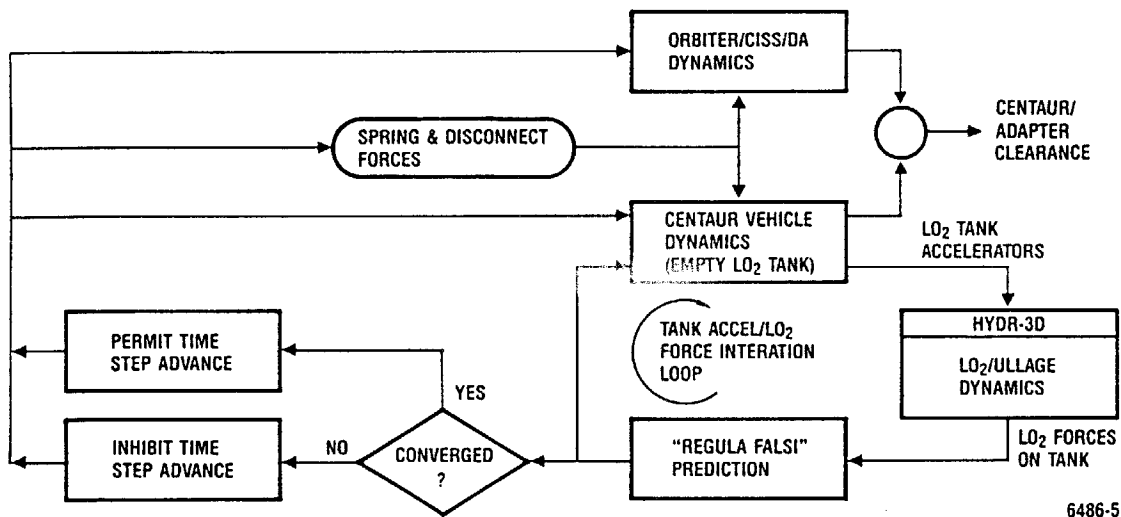


Fig. 2. Shuttle/Centaur separation simulation flow diagram.

It became apparent that the output accelerations of SEP must produce the output forces from HYDR-3D (and vice versa) within tight tolerances before the next integration time step involving other parameter changes could be made. The "Regula Falsi" technique (Conte and deBoor, 1972) was found to be usually successful. In this technique, three successive estimates of liquid force are made and convergence to compatibility with input acceleration within a set tolerance checked. If convergence is not achieved, a new estimate is made by extrapolating from the previous three. Only when the forces are converged are they handed to the full SEP vehicle model which integrates forward in time to "catch up with" HYDR-3D.

Occasionally, the automatic mesh generation will result in a boundary cell shape that, for a particular flow direction, has a large inflow area and small outflow area. This produces an unrealistic pressure "spike" which is reduced but not eliminated by the limited compressibility option in HYDR-3D. Particularly in periods of small liquid forces, these spikes made overall convergence difficult. For these periods a technique was devised to temporarily relax the convergence tolerance until the spike is passed and test "Regula Falsi" convergence based on absolute rather than percentage change in forces. This is an area that will likely produce different numerical problems for different applications and one worthy of further research.

The combined program has primarily been run on CDC-CYBER 855 and FPS-164 array processor computers. A typical seven-second, real-time simulation of clearance of the DA requires about 10,000 CPU seconds on the CYBER and 12,000 on the FPS. The most demanding case to date involved simulation of the drop-tower validation tests (described in the next section). In this case the very small scale greatly magnified the effects of surface tension and wall adhesion, requiring about 16,000 cells as opposed to 6,000 for a typical

full-scale simulation. This case (which did not require SEP) would not fit the above computers, and required 35,000 CPU seconds on a CRAY 1. Cost is highly dependent on a number of factors influencing each installation's cost algorithm, but in our case ranged from \$200 per run for the simplest planar simulation to \$10,000 for the most complex, full 3D simulation of the drop-tower test.

### HYDR-3D VALIDATION WITH TEST DATA

HYDR-3D had previously been shown to provide good correlation with slosh data obtained in a 1g acceleration field, as demonstrated by Sicilian and Hirt (1984). General Dynamics performed a similar comparison for the Centaur LO<sub>2</sub> tank for which complete slosh model test data is available. This correlation was also good.

Rockwell, Inc. has used an earlier version of HYDR-3D, SOLA-SLOSH, to compare with low-g test data obtained from KC-135 flights. A tank similar to the G-Prime LO<sub>2</sub> tank (approximately quarter-scale) was rotated 90 degrees during the low-g portion of the KC-135 maneuver and net fluid forces and moments determined from load cell measurements. Figure 3 is a schematic of the test apparatus. The KC-135 flew parabolas which produced about 30 seconds of near zero-g. The best runs maintained positive g's less than 0.02, resulting in initial fluid position similar to the lower tank position in Fig. 3. The rotation device accelerated the tank for 45 degrees and decelerated for 45 degrees to produce a 90 degree total rotation. The tanks were instrumented in all six degrees of freedom with accelerometers, gyros, and load cells to detect motion and forces. Post processing of the recorded data subtracted the effects of dry tank inertia so that resulting force and moment time histories were due solely to the liquid (water). The upper left chart in Fig. 6 shows the desired square-wave rotational acceleration and the actual which has a large superimposed 3Hz oscillation. The oscillation is the vibratory structural response of the support arm and torsion bar.

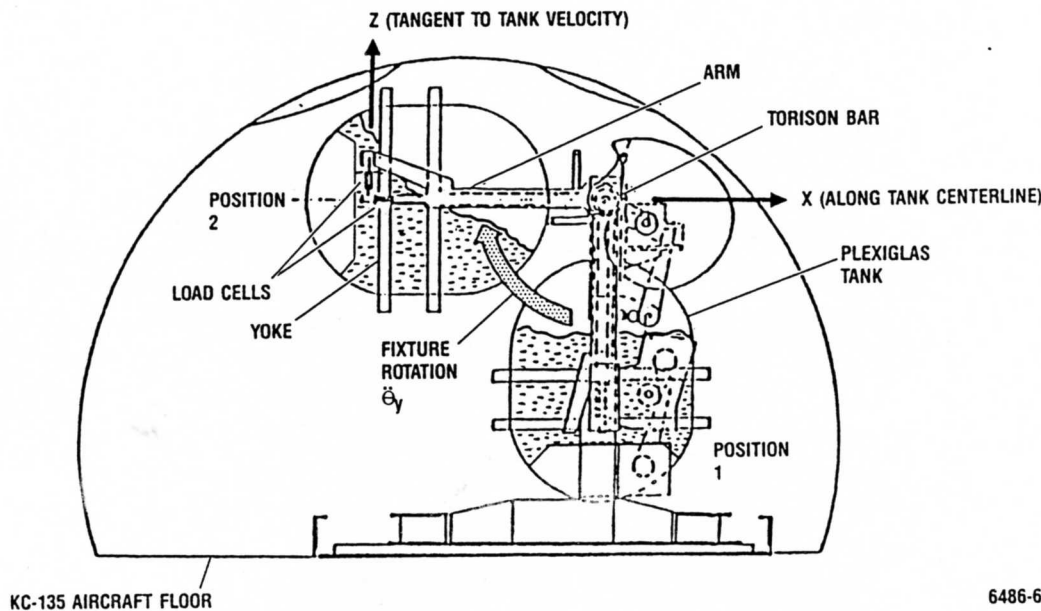


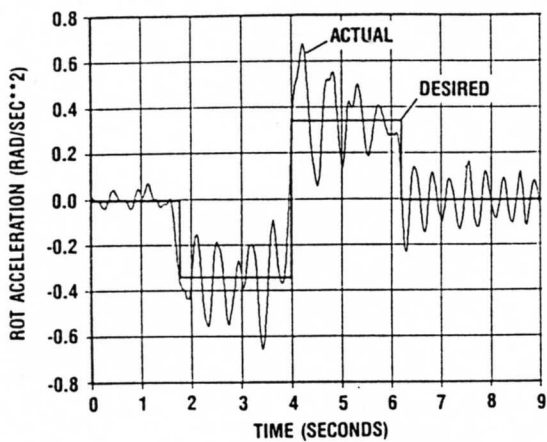
Fig. 3. Rotational test apparatus mounted in KC-135 aircraft.

The measured base and arm accelerations and rotational velocities were input to a HYDR-3D model of the tank via the MOTION subroutine. The other three charts of Fig. 4 compare the HYDR-3D with measured radial (X) and tangential (Z) forces and the net moment about the Y orthogonal axis through the load center. It is seen that HYDR-3D does a good job of predicting the time history forces and moments due to the rigid body motions and even a fair job of predicting the peaks due to the unwanted elastic body motions which would not be in the real situation. Rocketdyne (Estes, Chang, Hirt, and Sicilian, 1985) performed a similar correlation using SOLA-SLOSH and obtained equally good results.

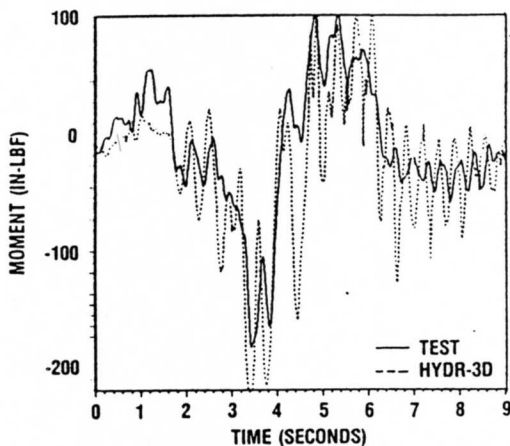
Further validation was obtained by comparing HYDR-3D ullage motion predictions with zero-g drop tower tests performed by NASA/Lewis Research Center. In this test a 1/76th scale Centaur G LO<sub>2</sub> tank was dropped, a spherical zero-g ullage bubble formed, and a lateral acceleration applied, simulating acceleration attributable to the separation springs. Figure 5 depicts the test approach. The only instrumentation possible was a movie camera to track the motion and shape of the ullage. The general behavior was for the acceleration to drive the ullage to the side of the tank (top in real vehicle), forming a geyser in the middle which formed the ullage into a toroidal shape. Figure 6 shows the peak of the geyser formation and a sketch interpreting the liquid/vapor interface. The photo in Fig. 6 is from a test with Ethanol as the fluid and 25 percent ullage. FC-43 liquid and 10 percent ullage were also tested. Careful interpretation was required by the LeRC engineer to distinguish distortion due to light refraction through the tank and support structure. Since the camera was fixed and the tank moved across it, corrections for parallax were also required. The test data reduction was done entirely by LeRC and not made available to the GDSSD engineer doing the HYDR-3D simulation until all results were complete. A detailed description of the test setup and fluid behavior is given by Aydelott and Carney (1985).

The measured acceleration time history and the initial ullage location and shape at the start of acceleration were used as input to the HYDR-3D model. A very detailed HYDR-3D model was required since the effects of surface tension and viscosity were greatly magnified by the small (2 cm x 1.47 cm) tank model. The parameters which should be scaled for this type transient fluid behavior are

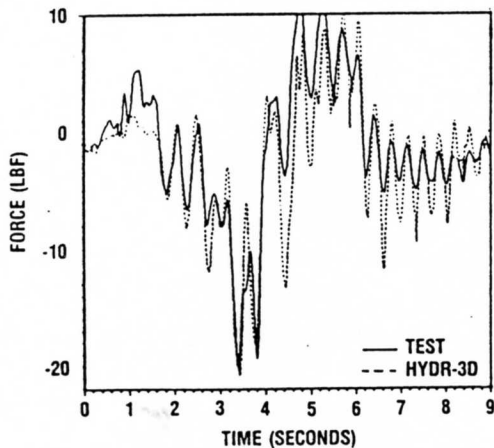
APPLIED TANK ROTAT ACCEL ABOUT Y THROUGH LOAD CENTER



MOMENT ABOUT Y THROUGH LOAD CENTER



RADIAL FORCE (X)



TANGENTIAL FORCE (Z)

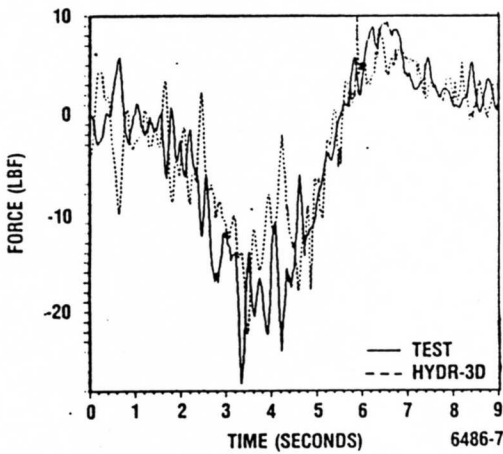
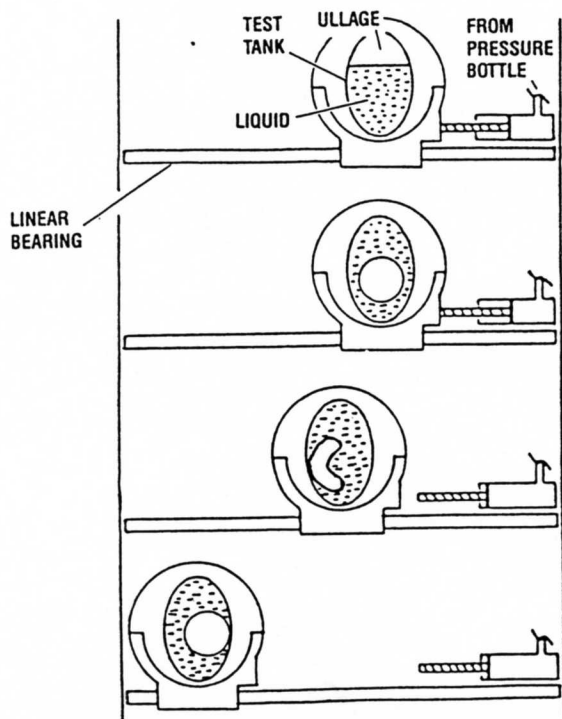


Fig. 4. Correlation of HYDR-3D with Rocketdyne KC-135 low-g measured forces and moment.



$t = 0$   
START DROP

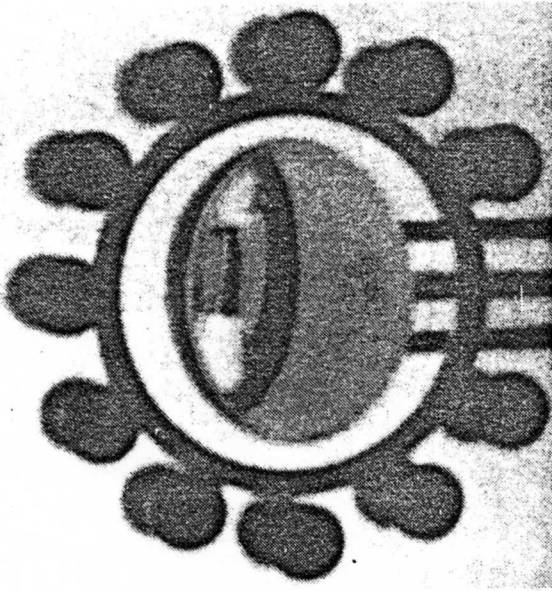
$t \approx 3.2$  SEC  
ZERO-G ULLAGE SHAPE HAS  
STABILIZED. LATERAL FORCE  
SIMULATING CENTAUR SEPARATION  
IS INITIATED

$t > 3.2$  SEC  
ULLAGE DEFORMATION  
TRANSIENT OCCURS

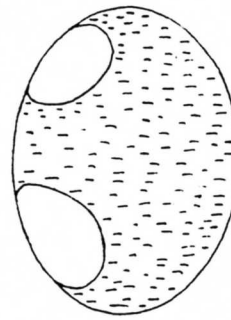
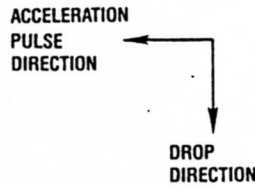
$t \approx 5$  SEC  
END OF RUN - TEST BED REACHES  
BOTTOM OF TOWER

6486-8

Fig. 5. Centaur-G LO<sub>2</sub> tank model drop test schematic.



PHOTO



INTERPRETATION

6486-10

Fig. 6. Typical drop test photo and interpretation (Ethanol liquid, 25% ullage,  $t = 0.15$  sec.)

Bond number (ratio of gravity to surface tension forces) during acceleration and Weber number (ratio of inertia to surface tension force) after removal of acceleration. The test Bond numbers ranged from 30 to 64, whereas typical full-scale is 344,000. Test Weber numbers ranged from 37 to 68 whereas full-scale is 38,200.

Figure 7 compares HYDR-3D with drop-tower test fluid/vapor interface curves at the center cross-section at three times: start of acceleration, during acceleration, and just after acceleration. It is seen that the formation of a geyser which distorts the ullage into a toroidal shape is accurately predicted by HYDR-3D. After a longer period of time (not of interest in the Centaur application), the test ullage recollected to a spherical shape whereas the HYDR-3D recollection was much more "ragged" and not in the same location. It was believed that an even finer cell grid and code modifications proposed by Flow Science would greatly improve the longer term ullage tracking, but cost and lack of application to the Centaur problem prevented further comparisons. The drop comparison was concluded to be an extreme test of the HYDR-3D capability and that its prediction of fluid forces during full-scale Centaur separation should be valid.

NASA/LeRC contracted Dr. John Hochstein to independently model the test with HYDR-3D. His results and conclusions (Hochstein, 1985) were the same as those of GDSSD. Further validation of HYDR-3D will be made against future Shuttle locker experiments on a 1/10th scale model of the Centaur G LO<sub>2</sub> tank sponsored by the USAF Space Division. Both single-pulse acceleration and jet-pulse mixing tests are to be performed.

#### CENTAUR SEPARATION RESULTS

The following summarizes key results of the coupled HYDR-3D/SEP simulation of Centaur G-Prime with the Galileo spacecraft separation from the Orbiter. Since it was concluded that the ullage location at separation could not be determined, an initial study evaluated the effects of ullage location in the LO<sub>2</sub> tank alone. The ullage volume is 11 percent of the total tank volume. Figure 8 depicts the trajectory of the outer edges of the aft end of the engine bells through the DA for four different assumed initial ullage locations. No guides or disturbances were used - only the axial acceleration due to springs and disconnects. A plus (or right) lateral displacement indicates the trajectory of the right side of the right engine toward the right side of the DA; a minus (or left) displacement of the left engine toward the left side of the DA. As expected, the zero degree (forward) initial ullage location resulted in a nearly straight out trajectory. It is not exactly so because the sum of the nominal axial impulses of all springs and disconnects results in a small net angular impulse. It was initially expected that 90 degrees would be the worst case because it produces the largest initial lateral center of mass (CM) offset. Figure 8 shows that this is not the case; the 45-degree location produces greatest loss of clearance.

Inspection of velocity patterns shows that during high velocity (high fluid force period) the 45-degree ullage (hence the CM) moves the most laterally while the 90-degree and 135-degree ullage move mostly axially. Figure 9 shows a typical migration and distortion of the ullage during the period of separation from the DA. It is clear that, although somewhat distorted, the ullage moves primarily as a whole and does not move much further once the disturbing separation and guide forces are removed. Neither has it had time to recollect by the time the DA is cleared. The peak velocity of any cell occurs at about 0.70 second, but by this time most of the gross migration is over. Of course, the greater the ullage percentage the greater the migration of both ullage and CM. It appears that the ullage gets smaller, but actually it is expanding perpendicular to the cross-section shown in Fig. 9.

Figure 10 shows clearance trajectories for the worst case expected (a root-sum-square of maximum tolerances) and for the worst dual-failure assumption required by safety. These curves represent envelopes of many simulations that vary key parameters, the primary parameters being initial ullage location and guide gap. The worst dual-failure scenario results in the LO<sub>2</sub> disconnect line (normally vented) being pressurized at separation. This creates a large angular impulse during the first 2 in. (0.25 second) of travel and large lateral forces on the guides (highly dependent on initial ullage location). In general (but with an occasional exception), the two

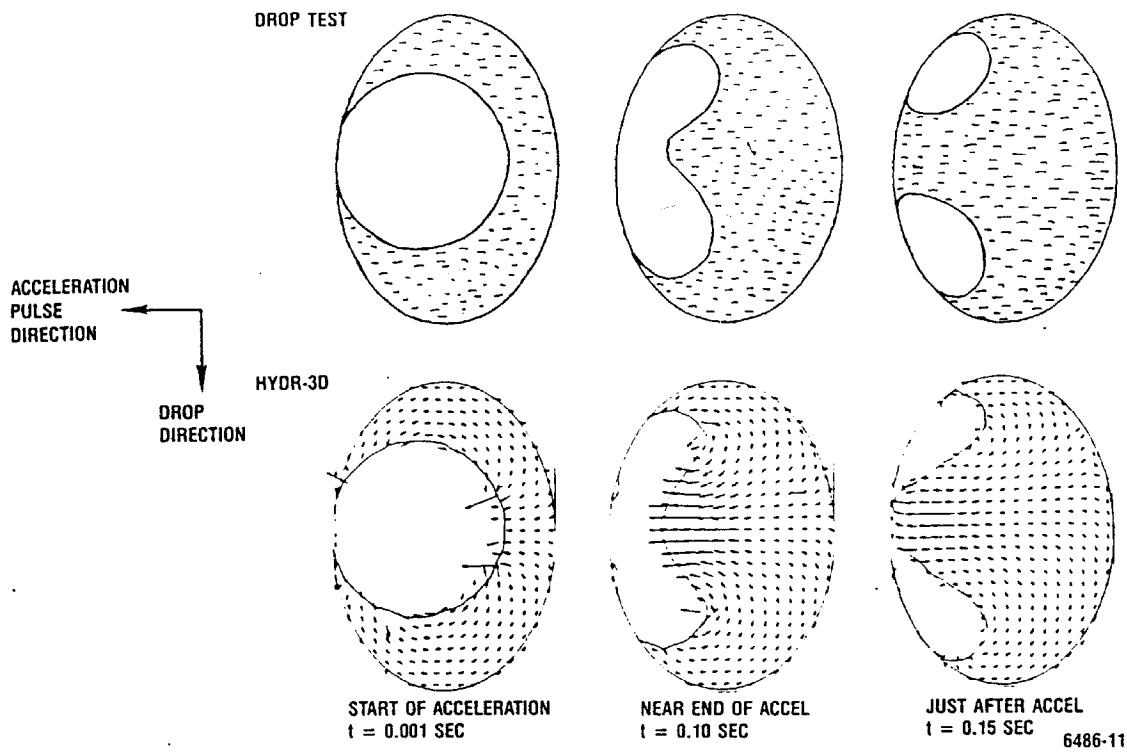


Fig. 7. Comparison of HYDR-3D and drop test liquid/vapor interface (Ethanol liquid, 25% ullage).

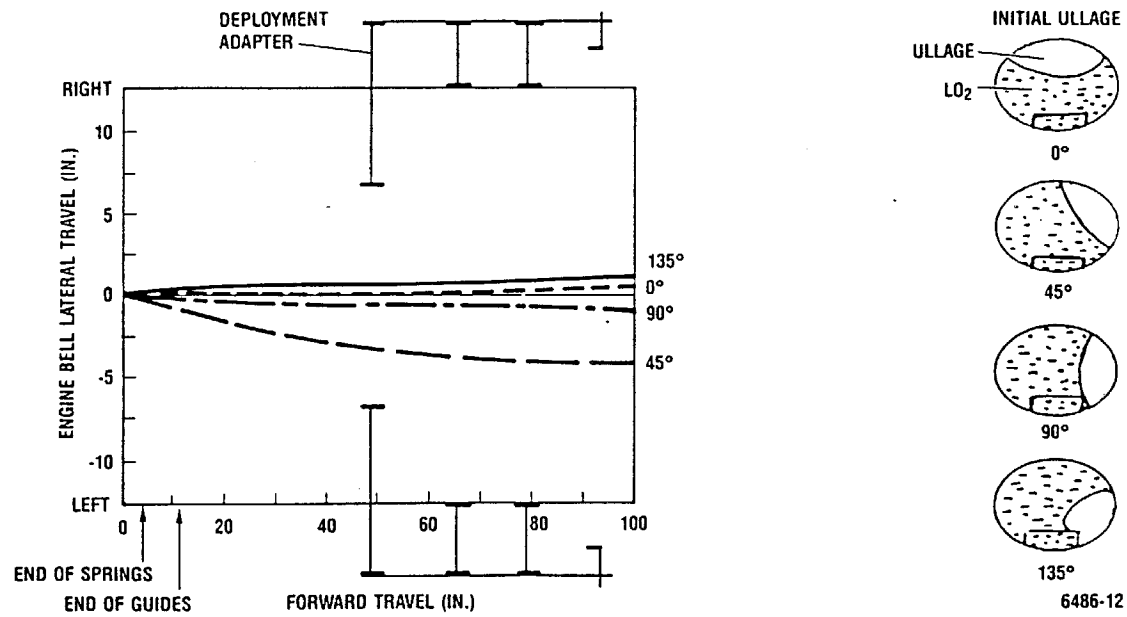


Fig. 8. Centaur/Galileo clearance loss due to initial ullage location.

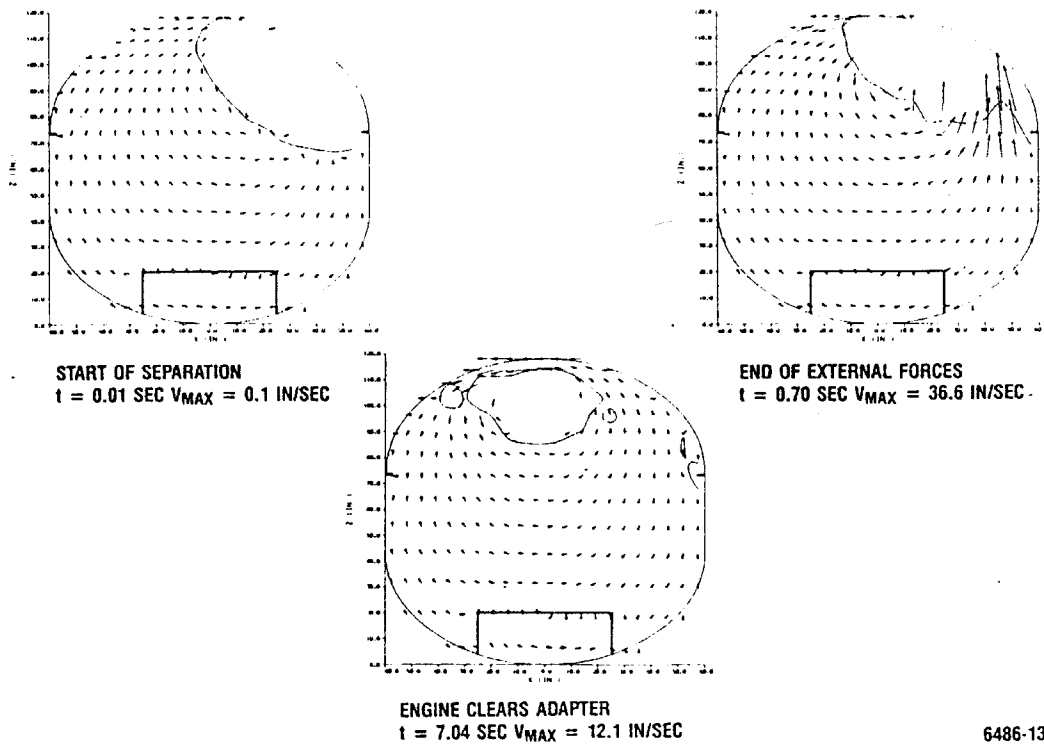


Fig. 9. G-Prime LO<sub>2</sub> velocity patterns during separation (11% ullage).

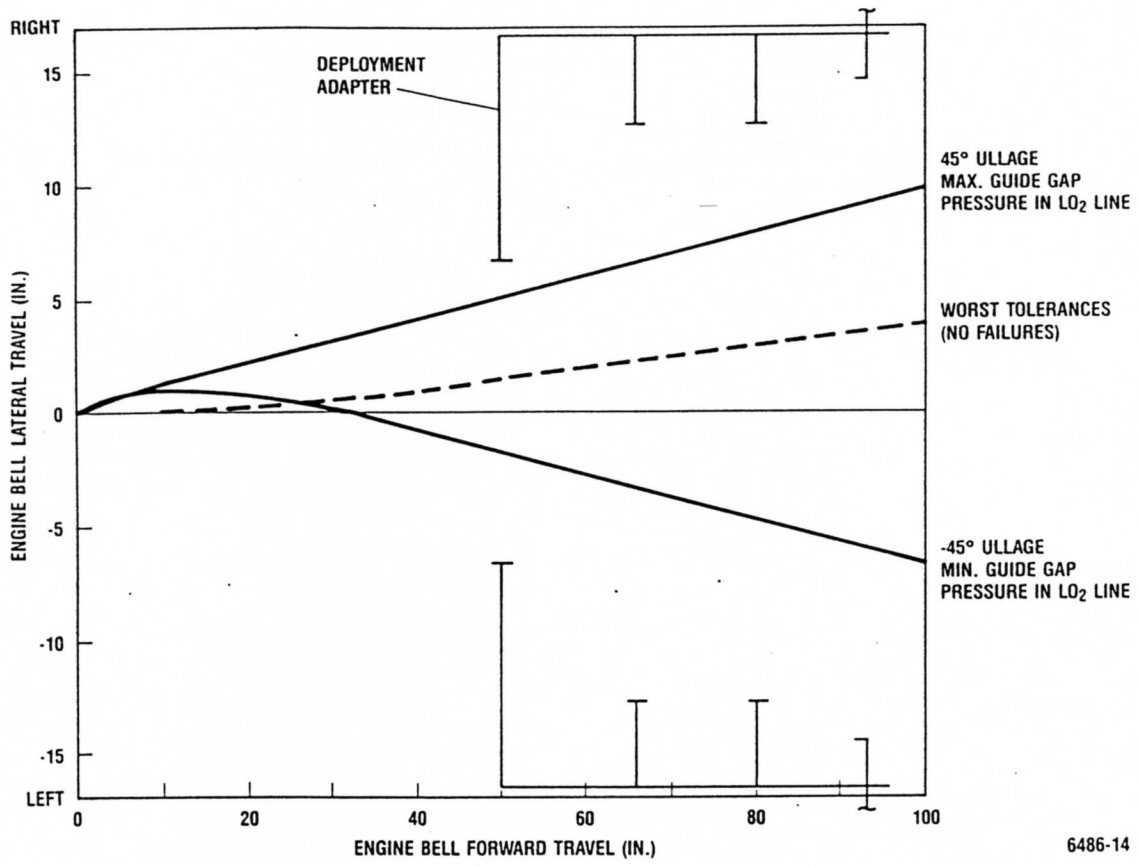
combinations of parameters shown for the dual failure in Fig. 10 produce the largest loss of clearance. The location of the LO<sub>2</sub> line produces a yaw left torque. The combination of ullage forward left (-45 degrees) and maximum guide gap results in fluid forces tending to reduce guide forces and minimize redirection by the guides. This is critical for the right engine since the yaw left torque will drive it to the right. The second critical combination is ullage forward right (+45 degrees) and minimum guide gap. This results in the net fluid torque acting in the same direction as the applied torque and maximum rebound off the guides. The initial rotation of the vehicle is reversed, and the left engine is critical. Although fluid dynamics have a significant effect, adequate clearance is achieved for the worst dual-failure scenario.

From a safety standpoint the prime issue is the possibility of Centaur contacting the Orbiter cabin, not engines bumping the deployment adapter. Figure 11 shows that, nominally, cabin clearance is very large (33 ft.) and that even after three failures (two separation springs plus Orbiter vernier control system) good clearance of 13.6 ft. is available. For cabin clearance, fluid dynamic effects are significant only in establishing the initial rotational rates coming off the guides.

Other contingency safety studies (they are not design requirements since they result from more than two failures) more dramatically illustrate the effect of tank propellant level and propellant dynamics on vehicle lateral motion during the separation transient. One such scenario requires an abort and dump of Centaur propellants in case of failures. However, the dump cannot be completed, and it is desired to jettison Centaur with whatever propellant remains. Taking the worst combination of parameters for largest lateral motion at different assumed LO<sub>2</sub> tank ullages (i.e. dump levels) results in the curve of engine lateral displacement versus percent ullage shown in Fig. 12. As expected, the 50 percent full case is most critical and causes much greater lateral travel than the normal case for Galileo of 11 percent ullage. Also shown is the equivalent data for Centaur G-Prime with the Ulysses spacecraft. Ulysses nominally can be loaded full to about half the ullage volume of Galileo, but it also is a much smaller spacecraft with about one half the moment of inertia. For nominal tank loading, these effects approximately offset each other. For abort dump conditions, the lower inertia of Ulysses significantly increases the loss of clearance. Although this contingency scenario would result in the engines contacting the DA, other analyses showed that this contact has a small effect on the trajectory of Centaur over the Orbiter cabin and is not a safety problem.

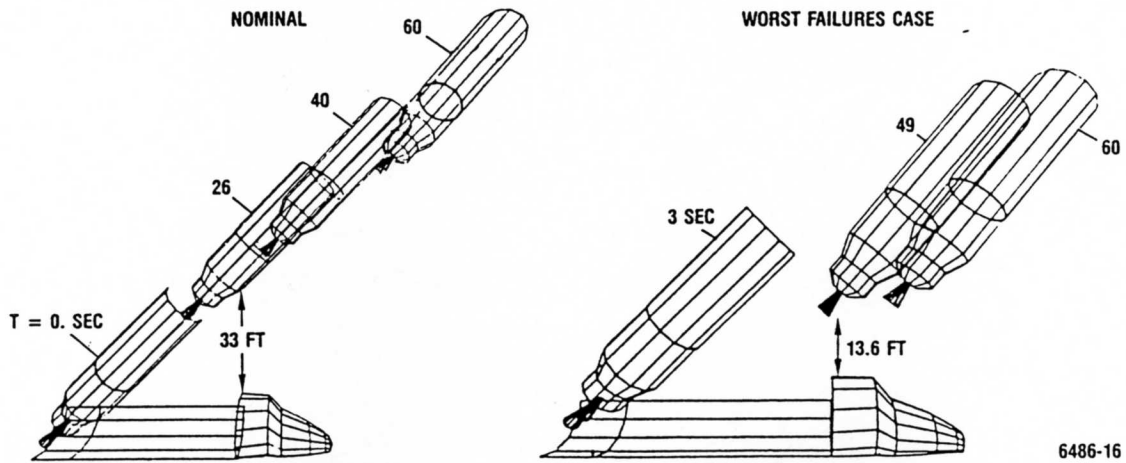
Another contingency studied for large offloads was use of the Orbiter attitude control jets to provide acceleration along the Centaur line of separation which settles propellants aft. This results in a forward ullage with a planar liquid/gas interface oscillating at slosh frequency. It was found that clearance loss was more sensitive to this ullage shape than the +45/-45 degree locations of the low-g ellipsoidal ullage bubbles. Allowable slosh angle at separation was found to be only about 12 degrees.





6486-14

Fig. 10. Centaur/Galileo clearance loss for worst combinations of ullage location, guide gap, and dual failures.



6486-16

Fig. 11. Centaur clearance of Orbiter cabin.

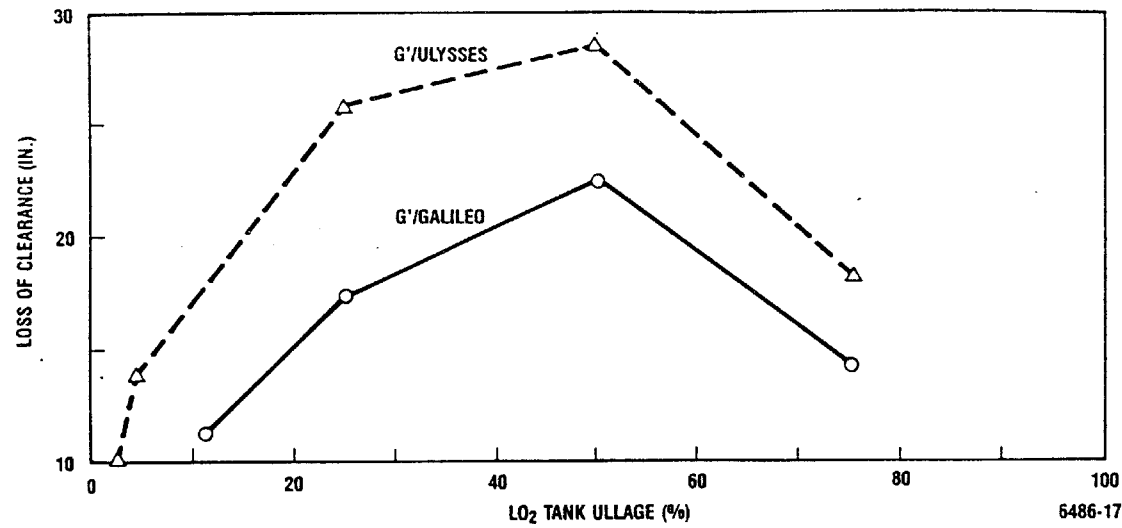


Fig. 12. Loss of clearance at forward ring of deployment adapter for abort dump conditions.

### CONCLUSIONS

Deployment or docking of large liquid propellant vehicles or storage tanks in space require accurate positioning which is highly influenced by the fluid dynamics. Until recently this zero-g, transient fluid dynamics problem was not analytically tractable. Adequate scale zero-g experimental data was not economically feasible.

Modern large-scale CFD capability, as represented by the Flow Science, Inc. HYDR-3D code, can analytically solve the fluid dynamics problem and has been adequately validated against small-scale low- and zero-gravity experimental data.

HYDR-3D coupled with detailed simulation of the vehicle dynamics can adequately evaluate the positioning problem and determine which design approaches are required. Detailed results from the Centaur/Orbiter separation simulation illustrate the effects of propellant dynamics on a large liquid upper stage. For this example results show that: 1) immediate clearance of the supporting deployment adapter is more critical than Orbiter cabin clearance, 2) the most critical clearance problem results from a multiple-failure condition requiring jettisoning with half-full propellant tanks, and 3) settling propellants before separation to reduce propellant dynamics effects on clearance must be done very precisely to be effective.

### ACKNOWLEDGEMENTS

This work was sponsored by the USA National Aeronautics and Space Administration/Lewis Research Center under Contract NAS-3-22901. It was a major team effort on which the author was the overall technical integrator. The vehicle dynamics effort was led by Dan Chiarappa with support from Luis Guevarra and Dan Robertson and programming by Louis Engbreghof. The integration of the vehicle dynamics with HYDR-3D was done by Noel Hughes, application and validation of HYDR-3D by Gary Steuber and Joe Fredley. Valuable consulting on the use of their HYDR-3D program was provided by Jim Sicilian and Tony Hirt of Flow Sciences, Inc. Valuable continuing critique and encouragement was provided by Ray Lacovic and the drop-tower test data by Mike Carney, both of NASA/LeRC. The assistance of the U.S. Air Force and Rocketdyne Division of Rockwell International, Inc. in providing the KC-135 test data is greatly appreciated.

### REFERENCES

- Carney, M.J. (1985) Liquid-Vapor Interface Locations in a Spheroidal Container Under Low-Gravity. NASA TM-87147.
- Hirt, C.W. and Sicilian, J.M. (1985a) HYDR-3D A Solution Algorithm for Transient 3D Flows. Flow Science, Inc. User's Manual FSI-84-00-3.
- Hirt, C.W. and Sicilian, J.W. (1985b) A Porosity Technique for the Definition of Obstacles in Rectangular Cell Meshes. Fourth International Conference on Numerical Ship Hydrodynamics.
- Estes, T.W., Chang, Y.M., Hirt, C.W., and Sicilian, J.W. (1985) Zero Gravity Slosh Analysis. 1985 ASME Winter Annual Meeting.
- Conte, S.D. and deBoor, C. (1972) Elementary Numerical Analysis, an Algorithmic Approach. McGraw-Hill Book Company, New York.
- Sicilian, J.M. and Hirt, C.W. (1984) Numerical Simulation of Propellant Sloshing for Spacecraft. 1984 ASME Winter Annual Meeting, Forum on Unsteady Flow, G00259.
- Aydellott, J.L. and Carney, M.J. (1985) NASA Lewis Research Center Low-Gravity Fluid Management Technology Program. AIAA/GNOS Third Annual Aerospace Technology Symposium.
- Hochstein, J.I. (1985) Computational Prediction of Propellant Motion During Separation of a Centaur G-Prime Vehicle from the Shuttle. Washington University (St. Louis) Report WU/CFDL-85/1.